ARTICLE

BIOTECHNOLOGY and BIOENGINEERING

A Three-Dimensional Computer Model Analysis of Three Hypothetical Biofilm Detachment Mechanisms

Jason D. Chambless, Philip S. Stewart

Center for Biofilm Engineering, and Department of Chemical and Biological Engineering, Montana State University–Bozeman, Bozeman, Montana 59717-3980; telephone: (406) 994-4770; fax: (406) 994-6098; e-mail: phil_s@erc.montana.edu

Received 25 October 2006; accepted 22 January 2007

Published online 1 February 2007 in Wiley InterScience (www.interscience.wiley.com). DOI 10.1002/bit.21363

ABSTRACT: Three hypothetical mechanisms of detachment were incorporated into a three-dimensional computer model of biofilm development. The model integrated processes of substrate utilization, substrate diffusion, growth, cell advection, and detachment in a cellular automata framework. The purpose of this investigation was to characterize each of the mechanisms with respect to four criteria: the resulting biofilm structure, the existence of a steady state, the propensity for sloughing events, and the dynamics during starvation. The three detachment mechanisms analyzed represented various physical and biological influences hypothesized to affect biofilm detachment. The first invoked the concept of fluid shear removing biomass that protrudes far above the surface and is therefore subjected to relatively large drag forces. The second pathway linked detachment to changes in the local availability of a nutrient. The third pathway simulated an erosive process in which individual cells are lost from the surface of a biofilm cell cluster. The detachment mechanisms demonstrated diverse behaviors with respect to the four analysis criteria. The height-dependant mechanism produced flat, steady state biofilms that lacked sloughing events. Detachment based on substrate limitation produced significant sloughing events. The resulting biofilm structures included distinct, hollow clusters separated by channels. The erosion mechanism produced neither a non-zero steady state nor sloughing events. A mechanism combining all three-detachment mechanisms produced mushroom-like structures. The dynamics of biofilm decay during starvation were distinct for each detachment mechanism. These results show that detachment is a critical determinant of biofilm structure and of the dynamics of biofilm accumulation and loss.

Biotechnol. Bioeng. 2007;97: 1573–1584.

KEYWORDS: biofilm; detachment; model; structure; starvation; sloughing

Introduction

Planktonic microorganisms are typically easily understood. They do not employ complicated or diverse methods of growth, are easily eradicated with antimicrobials or biocides, and do not demonstrate sophisticated mechanisms of dispersal. However, these same microorganisms often will attach to wetted surfaces and form biofilms. Biofilm formation affords protection from antimicrobial challenges (Mah and O'toole, 2001; Stewart and Costerton, 2001), the potential for metabolic cooperation between species (Hall-Stoodley et al., 2004), and relative stability of the physical and chemical environment. Likewise, microorganisms also will detach from biofilms and return to the planktonic state. Detachment, or dispersal, is an important process that allows an organism the possibility of traveling to and colonizing a new location. Detachment also balances growth and so determines the net accumulation of biomass on the surface. Detachment is surely a critical determinant of microbial ecology and activity in many natural and engineered environments where biofilms form (Rittmann, 1989; Stewart, 1993).

The motivation behind research on biofilm detachment varies widely. Detachment studies can focus on discovering new approaches for controlling detrimental biofilms (Van der Borden et al., 2005; Xavier et al., 2005), improving biological reactor design for treating wastewater (Eker and Kargi, 2006; Gonzalez-Brambila et al., 2006; Odegaard, 2006; van Loosdrecht and Salem, 2006), or developing insight into the metastasis of infections within the human body (Fux et al., 2004; Khardori and Yassien, 1995; Wilson et al., 2004).

The biological, chemical, and physical factors that drive detachment are complex and incompletely understood.

Correspondence to: P.S. Stewart

Contract grant sponsor: NIH
Contract grant number: R01GM067245-02

Some of the phenomena or cues that are probably involved in detachment mechanisms include: degradation of the extracellular polymeric substances (EPS) constituting the biofilm matrix (Allison et al., 1998; Kaplan et al., 2003), presence of excess nutrients (Sauer et al., 2004), absence of sufficient nutrients (Gjermansen et al., 2005; Hunt et al., 2004; Jackson et al., 2002; Sawyer and Hermanowicz, 1998) or oxygen (Thormann et al., 2005), production of an autocidal protein (Mai-Prochnow et al., 2006), production of biosurfactants (Boles et al., 2005; Davey et al., 2003; Schoolin et al., 2004), quorum sensing (Dow et al., 2003; Purevdorj-Gage et al., 2005; Rice et al., 2005; Vuong et al., 2004), regulation by the secondary messenger cyclic di-GMP (Gjermansen et al., 2006; Thormann et al., 2006), nitrosative stress (Barraud et al., 2006), hydraulic shear and normal forces (Guillemot et al., 2006; Liu and Tay, 2001; Manz et al., 2005), cation crosslinking (Banin et al., 2006; Chen and Stewart, 2002; Turakhia et al., 1983), sloughing (Applegate and Bryers, 1991; Howell and Atkinson, 1976; Telgmann et al., 2004), and erosive action (Bester et al., 2005; Gikas and Livingston, 2006; Nicolella et al., 1997). Judging from the length and variety of phenomena hypothesized as factors in biofilm detachment, one can anticipate that there are multiple detachment mechanisms, each of which may be multifactorial.

The absence of a single pathway to understanding biofilm detachment is reflected in the wide variety of mathematical submodels that have been proposed to describe detachment. It is worth noting that a number of important multidimensional biofilm models neglect detachment entirely (Eberl et al., 2001; Kreft et al., 2001; Noguera et al., 1999; Picioreanu et al., 1999; Wimpenny and Colasanti, 1997). Others neglect cells that move out of the model domain (Picioreanu et al., 1998, 2004) or consider detachment to be subsumed in a general decay process (Dockery and Klapper, 2001; Pizarro et al., 2001).

The earliest detachment models were those based on concepts of fluid shear (Peyton and Characklis, 1993; Rittmann, 1982) in which the rate of detachment increases with the distance above the substratum (Bryers, 1984; Trulear and Characklis, 1982; Wanner and Gujer, 1986). A common form assumes that detachment rate is proportional to the square of the height above the substratum, a functionality that has the practical advantage of ensuring a steady state (Stewart, 1993). Shear models of detachment in which a key variable is height continue to be widely and successfully employed in biofilm modeling (e.g., Xavier et al., 2005a,b). One particularly elegant model computationally solved the fluid hydrodynamics around the biofilm, calculated internal stresses in the biofilm treating the biofilm as an elastic solid, and allowed for biofilm detachment via adhesive or cohesive failure (Picioreanu et al., 2001).

A few biofilm models have made detachment rates dependent on the local concentration of a metabolic substrate or product. Several studies specifically link detachment to nutrient deprivation (Chambless et al., 2006; Hunt et al., 2004; Luna et al., 2004). Hunt et al. (2003) investigated biofilm dynamics using a detachment function that depended on the concentration of a metabolic product, an approach that simulates the hypothetical accumulation of a quorum sensing signal as an impetus for detachment. Xavier et al. (2005) implemented a detachment function that allowed for an externally added agent to degrade the mechanical cohesiveness of the biofilm matrix and thereby increase local detachment.

Some multidimensional biofilm models have prescribed an erosive detachment mechanism in which individual cells are lost from the surface of the biofilm (Hermanowicz, 2001; Laspidou and Rittmann, 2004). We note that 1D models of biofilm formation have never employed surface erosion models of detachment that are independent of height. The likely reason for this is that a purely erosive model cannot produce a non-zero steady state. The rate of erosion from a flat surface is constant. A biofilm that begins to grow when the simulation starts will continue to grow indefinitely. A biofilm that begins to erode away at the outset will decay away to a bare substratum. A relevant question is whether the same outcomes are expected in biofilm models of higher dimensionality.

In this study, we have focused on three conceptually distinct pathways of detachment. The first invokes the concept of fluid shear removing biomass that protrudes far above the surface and is therefore subjected to relatively large drag forces. The second pathway links detachment to changes in the local availability of a nutrient. The third pathway attempts to simulate an erosive process in which individual cells are lost from the surface of a biofilm cell cluster. Each detachment mechanism was investigated computationally using a hybrid cellular automata model called BacLAB. The purpose of this study was to characterize each of the hypothetical mechanisms with respect to four criteria: the resulting biofilm structure, the existence of a steady state, the propensity for sloughing events, and the behavior during starvation. The overall goal of this project was to compare the qualitative behaviors predicted in simulations using the three detachment mechanisms and to demonstrate that the choice of detachment mechanism can, by itself, profoundly influence biofilm structure and dynamics.

Materials and Methods

Description of BacLAB Model

The BacLAB computer model used in this investigation has been described in three prior publications (Chambless et al., 2006; Hunt et al., 2003, 2004). The model integrated processes of substrate utilization, substrate diffusion, microbial growth, advective displacement of biomass, and detachment in a cellular automata framework. The distribution of the soluble substrate was modeled using discretized differential equations describing simultaneous reaction and diffusion while the individual microorganisms

DOI 10.1002/bit

that compose the biofilm were modeled discretely using a cellular automata algorithm. A cellular automaton is an independent unit, here equated to a microbial cell and its associated matrix material, which follows certain behavioral rules. In BacLAB, a biofilm cell can occupy fixed nodes on a regular three-dimensional (3D) grid. When a cell has consumed sufficient substrate to divide, a daughter cell is generated and placed in an adjoining node. Growth can lead to the displacement of neighboring cells when there is no empty adjoining node to receive the daughter. This displacement is analogous to the process of biomass advection as articulated by Wanner and Gujer (1986). A cell can detach, in which case it is removed entirely from the model space. When a biofilm cell (or cluster of cells) no longer has an unbroken chain of occupied automata nodes leading back to the substratum, the cell (or cluster) is removed from the model space and considered to have detached. In this way it is possible for a single detaching cell to precipitate the release of an aggregate of cells. Neither fluid flow nor the EPS of the biofilm were explicitly included in the model. Cellular automata models can produce realistic, structurally heterogeneous biofilms (Chambless et al., 2006; Eberl et al., 2000; Hunt et al., 2004; Noguera et al., 1999; Picioreanu et al., 1998b). In these computer simulations, biofilm structure and activity evolve from the interactions between cells, emulating how bacterial cells organize themselves into biofilms. Parameter values are summarized in Table I. The following subsection explains the conceptual basis, and mathematical implementation, of each detachment mechanism explored in this study.

Mechanism Descriptions

Each detachment mechanism modeled here was based conceptually on a single factor hypothesized to influence detachment. The mechanisms were modeled individually to characterize their behavior with respect to the four criteria mentioned above. An additional analysis examined a mathematical description of detachment that combined the three individual mechanisms.

Shear Detachment

This mechanism is the classic model of biofilm detachment and reflects, in an empirical fashion, the influence of fluid shear (Bryers, 1984; Guillemot et al., 2006; Manz et al., 2005; Stewart, 1993). As the clusters of a biofilm grow taller, they are subjected to elevated shear forces from the movement of the bulk liquid. In order to simulate this effect, the probability of a cell detaching was made proportional to the square of its height above the substratum. The choice of squared dependence on height is empirical. We made this choice because this formulation has been used both in prior seminal 1D modeling studies (Wanner and Gujer, 1986) and in more recent 3D treatments (Xavier et al., 2005a,b). A squared dependence on height has the advantage of ensuring a steady state (Stewart, 1993). In mathematical terms the shear detachment relationship is given by:

$$P = K_S \cdot \Delta t \cdot \left(\frac{z}{Z_{max}}\right)^2 \quad (1)$$

where P is the probability of a given cell detaching, Δt is the length of each timestep, K_S is the detachment coefficient, z is the height of the biofilm cell, and Z_{max} is the maximum height allowed by the model. The inclusion of Z_{max} forces the growth of the biofilm to stay within the confines of the model space.

One of the conceptual barriers to using Equation (1) is that a cell deep in the interior of a cell cluster can detach. The probability of detachment depends only on height above the substratum, not on position within the biofilm structure. One can question how a cell can be ''sheared'' from the interior of a cell cluster without disturbing its neighbors. This is plainly not physically realistic at the individual cell level. On the other hand, a cell in the interior of a cell cluster can be removed by shear if it is stripped by fluid forces as part of an aggregate of cells. Modeling often involves simplifications that capture global properties of a phenomenon in ways that avoid undue complexity. The concept that cells that are further from the substratum are more likely to be detached is a reasonable concept, and Equation (1) implements this concept in a simple fashion.

Table I. Summary of parameters used in the BacLAB model.

Parameter	Symbol	Value	Unit(s)
Maximum specific growth rate	$\mu_{S,max}$	0.3	h^{-1}
Time step	Δt	1.0	h
Bulk substrate concentration	$C_{S,bulk}$	8.0	$g\,m^{-3}$
Diffusivity of substrate in aqueous phase (including the liquid, channels, and voids	$D_{S,aq}$	7.2×10^{-6}	$m^2\,h^{-1}$
Relative effective diffusivity of substrate in biofilm	$D_{S,e}/D_{S,aq}$	0.55	
Substrate Monod half saturation coefficient	K_M	0.1	$g\,m^{-3}$
Average cell mass	m_{avg}	1.75×10^{-13}	g
Initial number of colonies	N_c	28	
Number of nodes in x-direction	N_x	300	
Number of nodes in y-direction	N_y	300	
Radius of initial colonies	R_c	8.55×10^{-6}	m
Biomass yield (g_X) per gram of substrate (g_S)	Y_{XS}	0.24	$g_X\,g_S^{-1}$

Substrate Limited Detachment

The substrate limited mechanism simulates the possibility of deterioration of the biofilm in regions that are subjected to prolonged substrate limitation (Rice et al., 2005). This deterioration, and subsequent detachment, could be due to phenomena such as cell lysis or degradation of the extracellular matrix of the biofilm. We have not attempted to simulate the specifics of this pathway, as these remain uncertain. A simple timing function for cell detachment was implemented. When the local concentration of substrate around a biofilm cell dropped below a user-specified minimum ($C_{S,min}$) for an extended period of time (t_{detach}), the cell detached from the biofilm. We began our analysis with this version of the substrate limited detachment model because this is the detachment mechanisms that was implemented in two previous BacLAB studies (Chambless et al., 2006; Hunt et al., 2004). Later we describe a probabilistic variation of the substrate limited detachment model.

The substrate limited detachment mechanism can be expected to lead to detachment occurring from the interior of cell clusters where substrate concentrations are lowest. Here again is a physical paradox. How can a loose cell escape when it is surrounded by intact biofilm? It is perhaps most realistic to consider the early hollowing that occurs in a cell cluster to be due to cell lysis rather than detachment (Stewart et al., 2007; Webb et al., 2003). Later in the process, when the hollowed interior communicates with the bulk fluid, true detachment would be possible.

Erosion Detachment

The third mechanism addresses erosion. This mechanism focuses on the possibility of single cell detachment from the surfaces of the biofilm. In order to model this effect, the detachment probability of a cell was made inversely proportional to the number of neighboring cells. The equation used to determine detachment probabilities in this mechanism was:

$$P = K_e \cdot \Delta t \cdot \left(1 - \frac{n}{N_{max}}\right) \quad (2)$$

where P is the probability of detachment of an individual cell, Δt is the length of each timestep, K_e is the detachment coefficient, n is the cell's neighbor count, and N_{max} is the maximum number of neighbors possible. From this equation it is easily seen that only cells located at the biofilm-bulk fluid interface were able to detach. A condition for detachment within this mechanism is that the cell be surrounded by a minimum number of unoccupied nodes before detaching. A cell must have at least nine vacant nodes surrounding it, the equivalent of one completely exposed face, before detachment can occur.

The erosion detachment mechanism does not incorporate any influence of the exposure of the local biofilm surface to fluid shear. A cell at the top of a tall cell cluster that has five neighboring cells has the same probability of detaching as does a cell near the base of the biofilm that has five neighbors.

Table II. Parameter values related to each detachment mechanism.

Parameter	Symbol	Value	Unit(s)
Maximum height allowed by model	Z_{max}	256×10^{-6}	m
Starvation threshold concentration	$C_{s,min}$	0.1	$g\,m^{-3}$
Maximum number of neighbor cells	N_{max}	28	

The parameters related to each of the three detachment mechanisms are summarized in Table II.

Model Analysis

For each detachment mechanism, three experimental sets of simulations were performed: (1) the first set established the mechanism's ability to produce a steady state, and provided the resulting biofilm structure, using several rates of detachment, (2) the second set determined the propensity for sloughing events, and (3) the third set provided the results required to elucidate the behavior during starvation. The simulations in the first set of experiments were each controlled by a different rate of detachment respective to the particular mechanism. The number of simulations per experiment varied for each mechanism. A mechanism is said to have a steady state if it reaches a stable total cell density at some point during the simulation, and perturbations from this level are less than 5% of the total density over the next 100 h. For the second set of experiments, a single detachment rate was chosen from the first set and six replicate simulations were performed to determine the propensity for sloughing events. The definition of a sloughing event is the same as that used in our previous paper (Hunt et al., 2004), that is, greater than 50% of biomass removed in one time step. The third and final set of experiments used the same detachment rate as the second set, and also consisted of six replicates. Starvation conditions in this final set of experiments were applied when the biofilm reached a steady state by removing all substrate from the model space for the remainder of the simulation. Replicate simulations are employed due to the stochastic nature of the mechanisms and the model. Differences between replicate simulations arise, despite identical model parameter values, because of the random initial distribution of cells on the substratum, the random nature of cell displacement resulting from growth of neighboring cells, and the probabilistically driven detachment functions. Each simulation in each of the experimental sets ran for 500 h.

Two of the three mechanisms, erosion and shear, execute cell removal via a comparison between a calculated detachment probability and a random number. During each time step, all cells in the simulation generate a random

DOI 10.1002/bit

Figure 1. Typical simulation of biofilm development using the shear detachment mechanism. Microcolonies initially present merged into a confluent flat slab biofilm. This mechanism consistently produced biofilm structures lacking complex morphological features. Time is indicated in hours. [Color figure can be seen in the online version of this article, available at www.interscience.wiley.com.]

number from a uniform distribution on the interval [0,1]. If the calculated detachment probability is greater than this random number, and each of the other mechanism-specific conditions necessary for detachment are satisfied, the cell detaches from the biofilm. The final mechanism, substrate limitation, draws on a simple cause and effect relationship. Essentially, cells detach from the biofilm after they have been starved of substrate for a particular period of time.

Results

The purpose of this investigation was to characterize each of three hypothetical detachment mechanisms with respect to four criteria: the resulting biofilm structure, the existence of a steady state, the propensity for sloughing events, and the behavior during starvation. The results of this analysis are presented in this section.

Shear Detachment

Structure

Simulations of the shear detachment mechanism consistently produced flat slab biofilms (Fig. 1). Such features as clusters, towers, and channels were never observed in the steady-state structures. The height of the biofilm at steady state could be controlled by the value of the detachment coefficient (K_S).

Steady State

A clear steady state was consistently achieved in simulations tracking the overall biofilm cell count versus time (Fig. 2A).

Sloughing

Replicate simulations using a single value of the shear detachment coefficient exhibited a high degree of similarity, even though the initial cell count and colony placement were randomly determined (Fig. 2B). The biofilm grew exponentially until cells began to reach a particular height. Biofilm accumulation stalled at this height, creating a flat slab of cells. This mechanism showed no signs of sloughing.

Starvation

Biofilms generated by the shear detachment mechanism decayed in a uniform fashion when substrate was removed from the system (Fig. 2C). At hour 200 the model space was cleared of all substrate, and the biofilm immediately began to decay. As could be anticipated from a mechanism

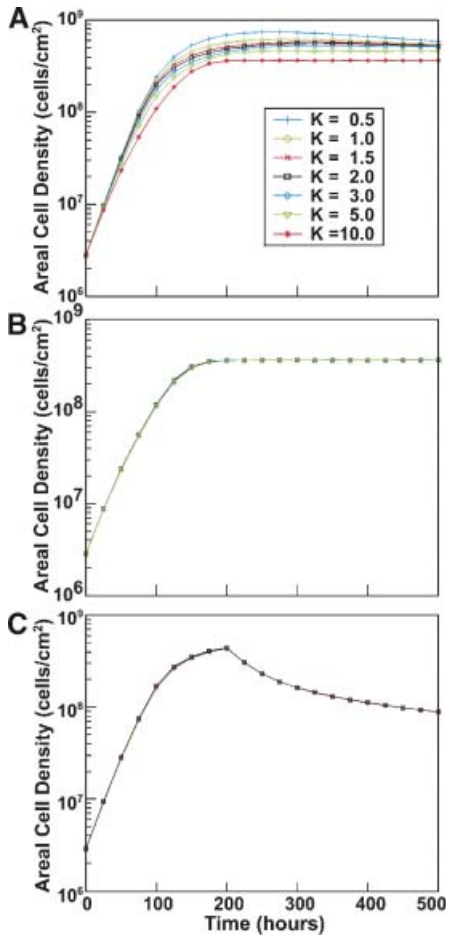

Figure 2. Seven simulations of the shear mechanism with seven different values of the detachment rate coefficient each provided a steady state cell density (**A**). Six replicate simulations of the shear mechanism with $K_S = 5.0$ showed zero sloughing events (**B**). Starvation conditions were introduced at hour 200 for each of six replicate simulations (**C**). This resulted in a decelerating, quadratic rate of decay that never completely removed the biofilm from the substratum. [Color figure can be seen in the online version of this article, available at www.interscience.wiley.com.]

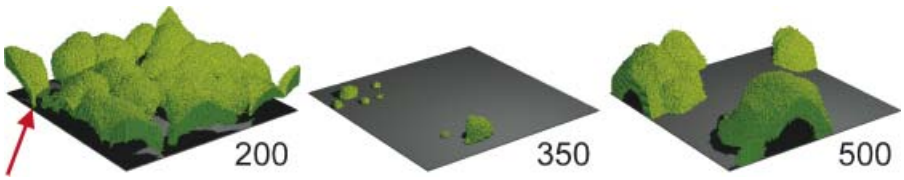

Figure 3. Typical simulation of biofilm development using the substrate limitation mechanism. These simulations produced towering, hollow structures that were loosely anchored to the substratum (red arrow) and that were prone to sloughing events. Biofilm growth renewed after sloughing events. Time is indicated in hours. [Color figure can be seen in the online version of this article, available at www.interscience.wiley.com.]

involving height-squared detachment, the decay was approximately quadratic. Again, no major sloughing events were observed, only a slow but steady decrease in the cell count. From the diminishing slope of the curve, it seems that this mechanism would predict extremely long starvation times in order to completely remove the biofilm. An additional simulation was performed to test this hypothesis. The end result showed that this mechanism did not exhibit complete removal even after 1,300 h of substrate starvation.

Substrate Limitation

Structure

The substrate limitation mechanism produced structures (Fig. 3) that were analogous to the swarming and hollow clusters found in some experimental studies (Boles et al., 2005; Kaplan et al., 2003b; Purevdorj-Gage et al., 2005; Stapper et al., 2004). Substrate limitation in the lower regions of the biofilm caused cells to detach, leaving hollow, towering clusters that were loosely tethered to the substratum. Hollow regions in time expanded to the point that they communicated with the bulk fluid. As the biofilms continued to grow taller and thus create diminished substrate concentrations near the substratum, nearly all cells in the lower strata of the biofilm detached due to limited availability of nutrients.

Steady State

Several detachment times (t_{detach}) were simulated with this mechanism, each one demonstrating a pseudo steady state (Fig. 4A). Please recall that t_{detach} is the period the local substrate concentration around a cell must be continuously below the minimum threshold concentration, $C_{S,min}$, before the cell detaches. A pseudo steady state is in effect when two cell densities separated by 100 h are within 5% of each other, despite the occurrence of sloughing events.

Sloughing

Replicate simulations using a single detachment time of 24 h each produced one or more major sloughing events, though the size and timing of the events were unpredictable (Fig. 4B). Bear in mind that the model's stochastic

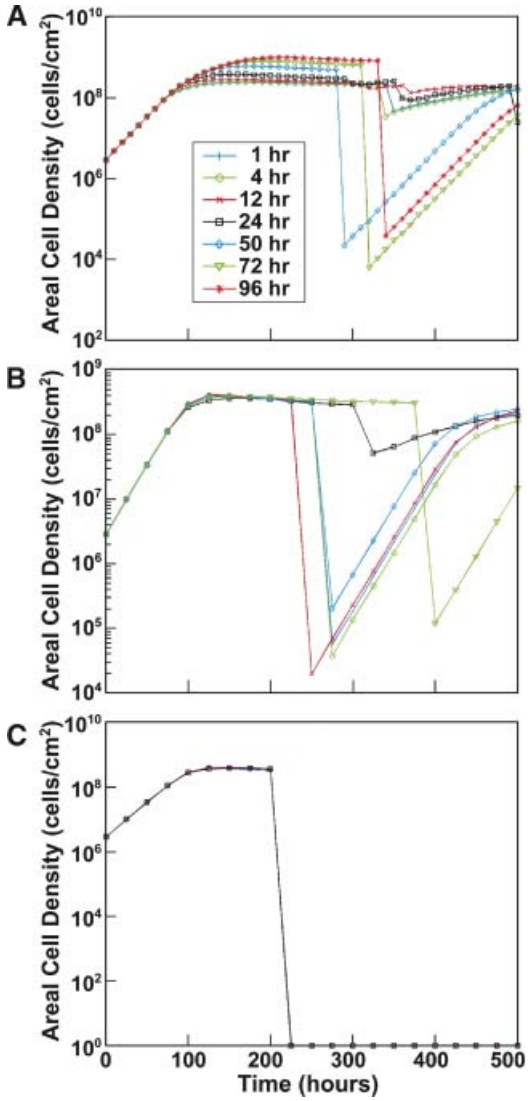

Figure 4. Seven simulations of the substrate limitation mechanism with seven different values of the detachment rate coefficient provided a pseudo steady state cell density despite the occurrence of sloughing events (**A**). Six replicate simulations using a single detachment time of 24 h each produced one or more major sloughing events, though the nature and timing of the event were unpredictable (**B**). Twenty-four hours after starvation conditions were imposed at 200 h, all cells simultaneously detached from the substratum (**C**), precluding the opportunity for regrowth. [Color figure can be seen in the online version of this article, available at www.interscience.wiley.com.]

DOI 10.1002/bit

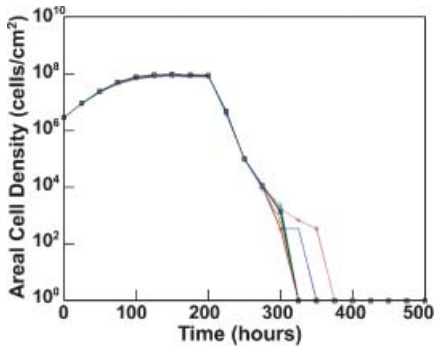

Figure 5. Response of biofilm formed using an alternative version of the substrate limitation detachment mechanism to starvation conditions. Six simulations of the substrate limitation mechanism were performed in which the detachment was not based on a timing function, but instead probabilistically tied to local substrate concentrations. Starvation conditions imposed at 200 h still lead to a steep loss of cell density, though less abrupt than the version presented in Figure 4C. [Color figure can be seen in the online version of this article, available at www.interscience.wiley.com.]

components allowed differences to arise in replicate simulations with equal parameters. The substrate limitation mechanism was the only mechanism to provide significant variability among the replicate simulations. An important observation is that none of the sloughing events led to complete removal of the biofilm.

Starvation

At hour 200 of each simulation shown in Figure 4C the model space was cleared of all substrate. The biofilm soon began to decay, and 24 h later, for each simulation, all cells simultaneously detached. Complete detachment precludes any chance of renewed growth if substrate were to be reintroduced. This extensive, sudden detachment may not be realistic. In order to further address this issue, we performed six additional simulations in which the detachment was not based on a timing function, but was instead probabilistically driven via a comparison between local substrate concentrations and the bulk substrate concentration. This version of the mechanism posited a higher probability of detachment for cells that were starved of substrate, as compared to those that had ample local substrate available. The equation describing this mechanism is:

$$P = K_{\text{sub}} \cdot \Delta t \cdot \left(1 - \frac{C_S}{C_{S,\text{bulk}}}\right) \tag{3}$$

where P is the probability of a cell detaching, K_{sub} is the detachment coefficient, Δt is the length of each timestep, C_S is the local substrate concentration for the cell, and $C_{S,\text{bulk}}$ is the bulk substrate concentration. This version of the substrate limited detachment still led to a steep loss of cell density during starvation, but the detachment was less abrupt (Fig. 5).

Erosion

Structure

The erosion mechanism produced tall, towering structures similar to those of the substrate limited mechanism, but did not demonstrate any signs of cluster hollowing (Fig. 6). Hollowing would not be expected since the inner cells are completely surrounded by neighbors, and, based on Equation (2), have a detachment probability of zero. The structures resemble confocal microscope images of *Pseudomonas aeruginosa* biofilms taken in some experimental studies (Klausen et al., 2003).

Steady State

The erosion mechanism did not produce a non-zero steady state. If the erosive detachment coefficient K_e was too large, the biofilm decayed completely; if it was too small, the biofilm achieved unrestricted growth (Fig. 7). Despite the intriguing structures produced by this mechanism, we did not attempt to analyze erosion detachment any further due to the inability of the mechanism to produce a steady state.

Combined Detachment Mechanism

After performing the starvation experiments with the probabilistic substrate limited mechanism, and in the

Figure 6. Typical simulation of biofilm development using the erosion mechanism. This detachment mechanism produced distinct towering structures. Unlike the clusters produced by the substrate limitation mechanism, no signs of cluster hollowing were observed. Time is indicated in hours. [Color figure can be seen in the online version of this article, available at www.interscience.wiley.com.]

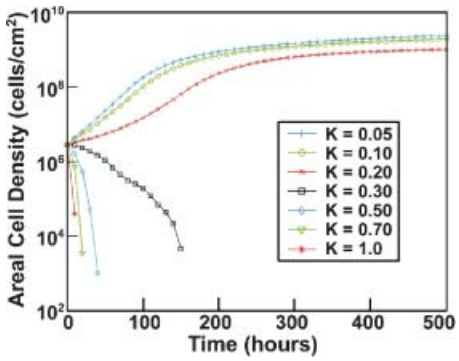

Figure 7. Seven simulations of biofilm development using the erosion detachment mechanism with different values of the detachment rate coefficient. The erosion mechanism did not produce a non-zero steady state. Some simulations decayed away to bare substratum while others achieved unrestricted growth. [Color figure can be seen in the online version of this article, available at www.interscience.wiley.com.]

interest of demonstrating that the erosion mechanism could be a contributing factor in biofilm detachment, we set out to learn what behavior would result from a combined mechanism that included the erosion, shear, and probabilistic substrate limitation mechanisms. The combined detachment was based on the summation of each separate mechanisms' probability of detachment, as shown in Equation (4):

$$P = \Delta t \cdot \left[K_S \cdot \left(\frac{z}{Z_{max}} \right)^2 + K_e \cdot \left(1 - \frac{n}{N_{max}} \right) + K_{sub} \cdot \left(1 - \frac{C_S}{C_{S,bulk}} \right) \right] \quad (4)$$

where each parameter definition is consistent with those in the previous three equations. All the conditional elements of the previous, separate simulations also applied in these simulations. In order to adequately combine these mechanisms, a single modification of the detachment probability was executed; namely, the detachment probability resulting from erosion was set equal to -1 if the cell did not meet the minimum vacant nodes criteria. Essentially, this modification provided a neighbor-based "cohesiveness" adjustment to the probability of detachment that severely decreased the likelihood of a cell detaching when it was surrounded by many neighboring cells. Also, to keep the number of simulations at an acceptable level the detachment coefficients were not varied individually; that is, all coefficients were equal during each particular simulation. Each simulation in each experimental set ran for 700 h.

Structure

Combining the three mechanisms generated tall, mushroom-like structures (Fig. 8), somewhat similar to those of the erosion mechanism. The mechanism featured towering clusters, minor sloughing events, and a "necking" phenomenon exemplified by thin stalks supporting large, spheroidal cell masses.

Steady State

Eight simulations were performed in this first experimental set, five of which reached a steady state (Fig. 9A). Simulations with coefficients equal to or greater than 0.35 decayed away before a stable cell count could be achieved. The simulation using a coefficient of 0.05 exceeded the upper limit of the model space, causing it to terminate before reaching 700 h.

Sloughing

Replicate simulations using detachment coefficients equal to 0.125 provided two instances of a sloughing event that removed 50% of the total biomass (Fig. 9B). Sloughing occurred in this mechanism due to the "necking" phenomenon, where the large mass of cells at the top of a cluster was released when the neck of the cluster pinched off (Fig. 10). Each simulation seemed to reach a maximum cell density, followed by a slow, natural decay resulting from an increase in substrate-limited- and erosion-driven cell removal at the bases of the biofilm clusters.

Starvation

Due to the late-occurring steady state of this mechanism, the starvation conditions were imposed at hour 400 instead of hour 200. With a detachment coefficient of 0.125 the shape of the starvation curve was concave down, indicating an

Figure 8. Typical simulation of biofilm development using the combined detachment mechanism. These simulations generated tall, mushroom-like structures that featured towering clusters, minor sloughing events, and a "necking" phenomenon exemplified by thin stalks supporting large, spherical cell masses (red arrows). Time is indicated in hours. [Color figure can be seen in the online version of this article, available at www.interscience.wiley.com.]

DOI 10.1002/bit

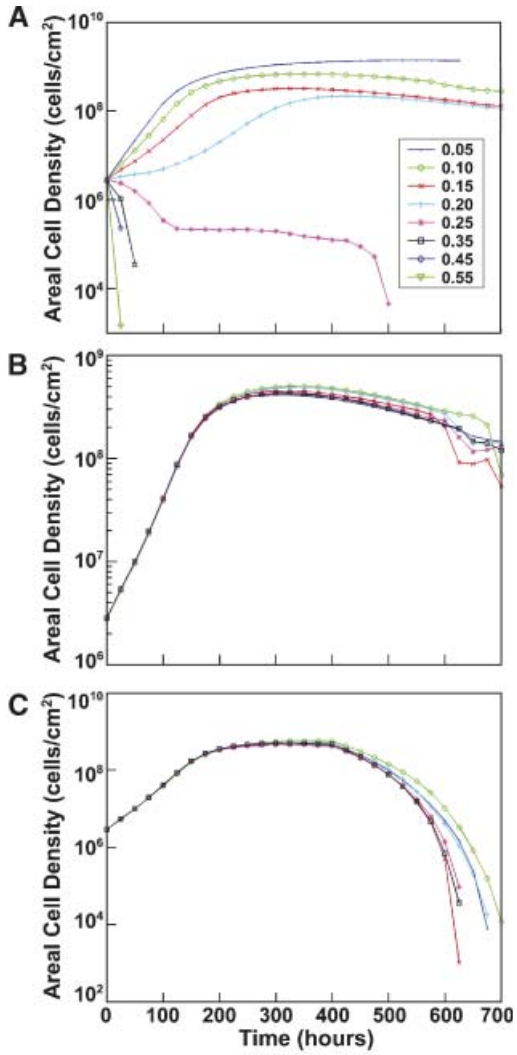

Figure 9. Eight simulations of the combined detachment mechanism with different values of the detachment rate coefficient. Five simulations reached a steady state, whereas simulations with coefficients greater than 0.25 decayed away (**A**). Two of the six replicate simulations using detachment coefficients equal to 0.125 produced a sloughing event of greater than 50% of the total biomass (**B**). Starvation conditions imposed at 400 h lead to concave down curvature in the cell density versus time trajectory, indicating an accelerating rate of attrition (**C**). All cells were eventually removed from the model space. [Color figure can be seen in the online version of this article, available at www.interscience.wiley.com.]

accelerating rate of attrition (Fig. 9C). Detachment during the starvation period caused several small sloughing events, along with the overall shrinking of all cell clusters. Complete cell removal was accomplished for each simulation within 330 h of the onset of starvation conditions.

Discussion and Conclusion

We have analyzed the simulated behavior resulting from four different mathematical descriptions of detachment incorporated in a 3D cellular automata biofilm model in which all other parameter values were held constant. Each

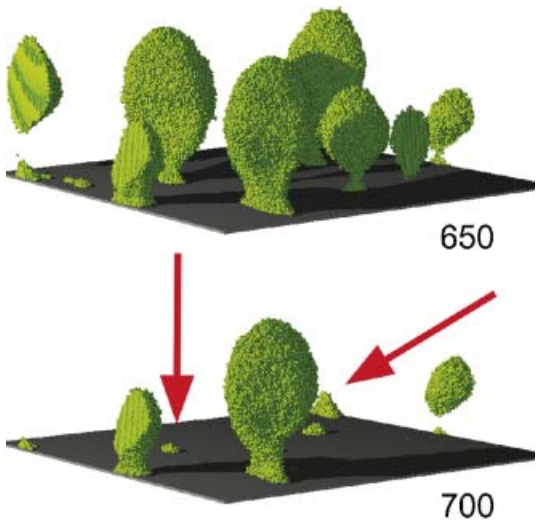

Figure 10. Example of a sloughing event in a simulation using the combined detachment mechanism. Sloughing occurred in this mechanism due to the "necking" phenomenon, where the large mass of cells at the top of a cluster was released when the neck of the cluster pinched off (location of detached cluster indicated by red arrows). Time is indicated in hours. [Color figure can be seen in the online version of this article, available at www.interscience.wiley.com.]

detachment mechanism resulted in distinct structural and dynamic features (Tab. III). One obvious conclusion is that the choice of specific detachment pathway alone can significantly influence biofilm structure and dynamic behavior. We are not aware of prior biofilm modeling studies that have performed such a side-by-side comparative analysis of different detachment models in which other parameter values are fixed.

Perhaps the most similar prior work to our study is that of Xavier et al. (2005). In that investigation, the authors demonstrated that a change in the magnitude of a single detachment rate coefficient could completely change the steady-state structure and dynamics of the biofilm. Hermanowicz (2001) also reported modest changes in biofilm structure predicted by a 2D model as the magnitude of a detachment coefficient was varied. The Xavier et al. report underscores the possibility that very different biofilm structures can arise with a single detachment mechanism. Thus, while we have demonstrated here that the specific detachment mechanism is important, there are other features of the system, such as the degree of external mass transfer resistance, that also influence biofilm structure.

It is surprising that many of the prior multidimensional biofilm modeling studies do not directly address the question of whether the model produces a steady state. A number of these studies do not include detachment at all (Eberl et al., 2001; Kreft et al., 2001; Noguera et al., 1999; Picioreanu et al., 1999; Wimpenny and Colasanti, 1997); a steady state is impossible. Others do not simulate detachment but rely on a subtractive decay process to balance growth (Dockery and Klapper, 2001; Pizarro et al., 2001). It is our contention that models in which detachment

Table III. Summary of results for each mechanism.

Mechanism	Structure	Existence of steady state	Propensity for sloughing	Starvation behavior
Shear	Flat slabs	Steady state achieved, regardless of the detachment coefficient	None	Quadratic, decelerating decay
Substrate Limitation	Towering clusters with hollow interiors, loosely anchored to the substratum	Pseudo-steady state, equal cell densities often separated by substantial sloughing events	Sloughing with seemingly random timing and size	All cells detached 24 h into starvation period
Erosion	Towering clusters with slight necking effects	No non-trivial steady state	Not tested	Not tested
Combined	Towering clusters with necking effects and base shrinkage	Steady state achieved with detachment coefficients less than or equal to $0.25h^{-1}$	Two sloughing events observed in six replicate simulations	Accelerating rate of decay leading to complete removal

occurs purely by surface erosion and is made independent of the distance above the substratum (e.g., Hermanowicz, 2001; Laspidou and Rittmann, 2004; and our erosion mechanism) cannot attain a non-zero steady state. This is based on the expectation that the surface area to volume ratio of biomass in the biofilm is greatest in the early stages of cell attachment and erosion will be proportionally large at this early stage. If the biofilm enlarges from this stage, it will continue to do so. There are two elegant, multidimensional modeling studies that address long-term behavior and demonstrate the potential for a noisy steady-state (Picioreanu et al., 2001; Xavier et al., 2005).

We have characterized the dynamic behavior of simulated biofilms in response to starvation, an analysis of which we are aware of no precedent in the literature. In starvation mode, growth is eliminated and the dynamic behavior is determined by detachment and decay processes alone. We suggest that this may be an informative experimental design for gathering clues about the nature of the detachment process. For example, it might be possible to discriminate between detachment dominated by a shear pathway and detachment dominated by a substrate limitation pathway with a starvation experiment. In starvation mode, our simulations suggest that the rate of biomass loss continually slows with a shear mechanism, whereas the rate continually increases with a substrate limitation mechanism.

We conclude with a few additional remarks about the three primary detachment mechanisms investigated in this work, beginning with the shear mechanism. The explanation for the lack of sloughing events observed with this detachment pathway is presumably that the detachment probability of individual cells near the substratum is so small, due to their low height, that the chance of an entire group of these cells simultaneously detaching is miniscule. A biofilm in which detachment is governed by a height-dependant shear mechanism could be particularly difficult to remove completely using antimicrobial and physical treatments. As the biofilm gets thinner, the rate of detachment slows and the residual biomass will persist.

The substrate limitation detachment mechanism produced hollow cell clusters and, later, cell clusters that were held to the substratum through thin contacts at the periphery of cluster. As the biofilm matures, cells in the deep interior of cell clusters are the first to experience prolonged substrate limitation and hence the first to detach. It may be appropriate to think of these lost cells as having lysed rather than detached since there is no path for physical release of cells from the interior of the cluster to the bulk fluid at the early stages of the hollowing process. As the biofilm continues to mature, however, the hollow interior expands until it communicates with the bulk fluid. Cells at the edge of the cell cluster, including those very close to the substratum have more substrate and are somewhat less likely to detach. This leads to the formation of umbrella-shaped structures that are loosely tethered at a few contact points around the edge of the cell cluster. The substrate limitation mechanism gives rise to sloughing events when these structures finally detach as one unit. Significant sloughing events were only observed when substrate limitation was included in the detachment model.

The erosion mechanism implemented in this study was independent of height above the substratum. This is likely an inadequate and unrealistic formulation. As discussed above, a purely erosive mechanism does not lead to non-zero steady states. When implemented in combination with height dependence, erosion detachment can lead to necked towers or mushrooms as described by Xavier et al. (2005b) and as shown in Figure 10. This shape arises when a cell cluster becomes tall enough that the lower portions of the cluster are substrate limited and therefore little new growth occurs. In these mid-portions of the cluster, erosion will cause the cluster to thin, generating a mushroom. Even though models generate mushroom-shaped structures resembling those seen by experimenters, this does not prove that this is the actual mechanism of formation of such structures.

This work was supported by NIH awards R01GM067245-02 to PSS and by an award from the W. M. Keck Foundation.

References

Allison DG, Ruiz B, SanJose C, Jaspe A, Gilbert P. 1998. Extracellular products as mediators of the formation and detachment of Pseudomonas fluorescens biofilms. FEMS Microbiol Lett 167(2):179–184.

Applegate DH, Bryers JD. 1991. Effects of carbon and oxygen limitations and calcium concentrations on biofilm removal processes. Biotechnol Bioeng 37(1):17–25.

DOI 10.1002/bit

Banin E, Brady KM, Greenberg EP. 2006. Chelator-induced dispersal and killing of Pseudomonas aeruginosa cells in a biofilm. Appl Environ Microbiol 72(3):2064–2069.

Barraud N, Hassett DJ, Hwang S-H, Rice SA, Kjelleberg S, Webb JS. 2006. Involvement of nitric oxide in biofilm dispersal of Pseudomonas aeruginosa. J Bacteriol 188:7344–7353.

Bester E, Wolfaardt G, Joubert L, Garny K, Saftic S. 2005. Planktonic-cell yield of a pseudomonad biofilm. Appl Environ Microbiol 71(12):7792–7798.

Boles BR, Thoendel M, Singh PK. 2005. Rhamnolipids mediate detachment of Pseudomonas aeruginosa from biofilms. Mol Microbiol 57(5):1210–1223.

Bryers JD. 1984. Biofilm formation and chemostat dynamics—Pure and mixed culture considerations. Biotechnol Bioeng 26(8):948–958.

Chambless JD, Hunt SM, Stewart PS. 2006. A three-dimensional computer model of four hypothetical mechanisms protecting biofilms from antimicrobials. Appl Environ Microbiol 72(3):2005–2013.

Chen X, Stewart PS. 2002. Role of electrostatic interactions in cohesion of bacterial biofilms. Appl Microbiol Biotechnol 59(6):718–720.

Davey ME, Caiazza NC, O'Toole GA. 2003. Rhamnolipid surfactant production affects biofilm architecture in Pseudomonas aeruginosa PAO1. J Bacteriol 185(3):1027–1036.

Dockery J, Klapper I. 2001. Finger formation in biofilm layers. SIAM J Appl Math 62:853–869.

Dow JM, Crossman L, Findlay K, He YQ, Feng JX, Tang JL. 2003. Biofilm dispersal in Xanthomonas campestris is controlled by cell-cell signaling and is required for full virulence to plants. Proc Nat Acad Sci 100(19):10995–11000.

Eberl HJ, Picioreanu C, Heijnen JJ, van Loosdrecht MCM. 2000. A three-dimensional numerical study on the correlation of spatial structure, hydrodynamic conditions, and mass transfer and conversion in biofilms. Chem Eng Sci 55(24):6209–6222.

Eberl HJ, Parker DF, van Loosdrecht MCM. 2001. A new deterministic spatio-temporal continuum model for biofilm development. J Theor Med 3:161–175.

Eker S, Kargi F. 2006. Biological treatment of para-chlorophenol containing synthetic wastewater using rotating brush biofilm reactor. J Hazard Mater 135(1–3):365–371.

Fux CA, Wilson S, Stoodley P. 2004. Detachment characteristics and oxacillin resistance of Staphyloccocus aureus biofilm emboli in an in vitro catheter infection model. J Bacteriol 186(14):4486–4491.

Gikas P, Livingston AG. 2006. Investigation of biofilm growth and attrition in a three-phase airlift bioreactor using (SO42-)-S-35 as a radiolabelled tracer. J Chem Tech Biotech 81(6):858–865.

Gjermansen M, Ragas P, Sternberg C, Molin S, Tolker-Nielsen T. 2005. Characterization of starvation-induced dispersion in Pseudomonas putida biofilms. Environ Microbiol 7(6):894–906.

Gjermansen M, Ragas P, Tolker-Nielsen T. 2006. Proteins with GGDEF and EAL domains regulate Pseudomonas putida biofilm formation and dispersal. FEMS Microbiol Lett 265:215–224.

Gonzalez-Brambila M, Monroy O, Lopez-Isunza F. 2006. Experimental and theoretical study of membrane-aerated biofilm reactor behavior under different modes of oxygen supply for the treatment of synthetic wastewater. Chem Eng Sci 61(16):5268–5281.

Guillemot G, Vaca-Medina G, Martin-Yken H, Vernhet A, Schmitz P, Mercier-Bonin M. 2006. Shear-flow induced detachment of Saccharomyces cerevisiae from stainless steel: Influence of yeast and solid surface properties. Colloids Surf B Biointerfaces 49(2):126–135.

Hall-Stoodley L, Costerton JW, Stoodley P. 2004. Bacterial biofilms: From the natural environment to infectious diseases. Nat Rev Microbiol 2(2):95–108.

Hermanowicz SW. 2001. A simple 2D biofilm model yields a variety of morphological features. Math Biosci 169:1–14.

Howell JA, Atkinson B. 1976. Sloughing of microbial film in trickling filters. Water Res 10:307–315.

Hunt SM, Hamilton MA, Sears JT, Harkin G, Reno J. 2003. A computer investigation of chemically mediated detachment in bacterial biofilms. Microbiol 149:1155–1163.

Hunt SM, Werner EM, Huang BC, Hamilton MA, Stewart PS. 2004. Hypothesis for the role of nutrient starvation in biofilm detachment. Appl Environ Microbiol 70(12):7418–7425.

Jackson DW, Suzuki K, Oakford L, Simecka JW, Hart ME, Romeo T. 2002. Biofilm formation and dispersal under the influence of the global regulator CsrA of Escherichia coli. J Bacteriol 184(1):290–301.

Kaplan JB, Ragunath C, Ramasubbu N, Fine DH. 2003. Detachment of Actinobacillus actinomycetemcomitans biofilm cells by an endogenous beta-hexosaminidase activity. J Bacteriol 185(16):4693–4698.

Kaplan JB, Meyenhofer MF, Fine DH. 2003b. Biofilm growth and detachment of Actinobacillus actinomycetemcomitans. J Bacteriol 185(4):1399–1404.

Khardori N, Yassien M. 1995. Biofilms in device-related infections. J Ind Microbiol 15:141–147.

Klausen M, Aaes-Jorgensen A, Molin S, Tolker-Nielsen T. 2003. Involvement of bacterial migration in the development of complex multicellular structures in Pseudomonas aeruginosa biofilms. Mol Microbiol 50(1):61–68.

Kreft J-U, Picioreanu C, Wimpenny JWT, van Loosdrecht MCM. 2001. Individual-based modeling of biofilms. Microbiology 147:2897–2912.

Laspidou CS, Rittmann BE. 2004. Modeling the development of biofilm density including active bacteria, inert biomass, and extracellular polymeric substances. Water Res 38:3349–3361.

Liu Y, Tay JH. 2001. Detachment forces and their influence on the structure and metabolic behaviour of biofilms. World J Microbiol Biotechnol 17(2):111–117.

Luna E, Dominguez-Zacarias G, Ferreira CP, Velasco-Hernandez JX. 2004. Detachment and diffusive-convective transport in an evolving heterogeneous two-dimensional biofilm hybrid model. Phys Rev E 70(6).

Mah TFC, O'toole GA. 2001. Mechanisms of biofilm resistance to antimicrobial agents. Trends Microbiol 9(1):34–39.

Mai-Prochnow A, Webb JS, Ferrari BC, Kjelleberg S. 2006. Ecological advantages of autolysis during the development and dispersal of Pseudoalteromonas tunicata biofilms. Appl Environ Microbiol 72(8):5414–5420.

Manz B, Volke F, Goll D, Horn H. 2005. Investigation of biofilm structure, flow patterns and detachment with magnetic resonance imaging. Wat Sci Technol 52(7):1–6.

Nicolella C, Chiarle S, DiFelice R, Rovatti M. 1997. Mechanisms of biofilm detachment in fluidized bed reactors. Wat Sci Technol 36(1):229–235.

Noguera DR, Pizarro G, Stahl DA, Rittmann BE. 1999. Simulation of multispecies biofilm development in three dimensions. Wat Sci Technol 39(7):123–130.

Odegaard H. 2006. Innovations in wastewater treatment: The moving bed biofilm process. Wat Sci Technol 53(9):17–33.

Peyton BM, Characklis WG. 1993. A statistical-analysis of the effect of substrate utilization and shear-stress on the kinetics of biofilm detachment. Biotechnol Bioeng 41(7):728–735.

Picioreanu C, van Loosdrecht MCM, Heijnen JJ. 1998. A new combined differential-discrete cellular automaton approach for biofilm modeling: Application for growth in gel beads. Biotechnol Bioeng 57(6):718–731.

Picioreanu C, van Loosdrecht MCM, Heijnen JJ. 1998b. Mathematical modeling of biofilm structure with a hybrid differential-discrete cellular automaton approach. Biotechnol Bioeng 58(1):101–116.

Picioreanu C, van Loosdrecht MCM, Heijnen JJ. 1999. Discrete-differential modelling of biofilm structure. Wat Sci Technol 39:115–122.

Picioreanu C, van Loosdrecht MCM, Heijnen JJ. 2001. Two-dimensional model of biofilm detachment caused by internal stress from liquid flow. Biotechnol Bioeng 72(2):205–218.

Picioreanu C, Kreft J-U, van Loosdrecht MCM. 2004. Particle-based multidimensional multispecies biofilm model. Appl Environ Microbiol 70:3024–3040.

Pizarro G, Griffeath D, Noguera DR. 2001. Quantitative cellular automaton model for biofilms. J Environ Eng ASCE 127(9):782–789.

Purevdorj-Gage B, Costerton WJ, Stoodley P. 2005. Phenotypic differentiation and seeding dispersal in non-mucoid and mucoid Pseudomonas aeruginosa biofilms. Microbiol 151:1569–1576.

Rice SA, Koh KS, Queck SY, Labbate M, Lam KW, Kjelleberg S. 2005. Biofilm formation and sloughing in Serratia marcescens are

controlled by quorum sensing and nutrient cues. J Bacteriol 187(10):3477–3485.
Rittmann BE. 1982. The effect of shear-stress on biofilm loss rate. Biotechnol Bioeng 24(2):501–506.
Rittmann BE. 1989. Detachment from biofilms. In: Characklis WG, Wilderer PA, editors. Structure and function of biofilms. New York, NY: John Wiley & Sons. p 49–58.
Sauer K, Cullen MC, Rickard AH, Zeef LAH, Davies DG, Gilbert P. 2004. Characterization of nutrient-induced dispersion in Pseudomonas aeruginosa PAO1 biofilm. J Bacteriol 186(21):7312–7326.
Sawyer LK, Hermanowicz SW. 1998. Detachment of biofilm bacteria due to variations in nutrient supply. Water Sci Technol 37(4–5):211–214.
Schoolin SR, Charaf UK, Allison DG, Gilbert P. 2004. A role for rhamnolipid in biofilm dispersion. Biofilms 1:91–99.
Stapper AP, Narasimhan G, Ohman DE, Barakat J, Hentzer M, Molin S, Kharazmi A, Hoiby N, Mathee K. 2004. Alginate production affects Pseudomonas aeruginosa biofilm development and architecture, but is not essential for biofilm formation. J Med Microbiol 53(7):679–690.
Stewart PS. 1993. A model of biofilm detachment. Biotechnol Bioeng 41(1):111–117.
Stewart PS, Costerton JW. 2001. Antibiotic resistance of bacteria in biofilms. Lancet 358(9276):135–138.
Stewart PS, Abdul Rani S, Gjersing E, Codd SL, Zheng Z, Pitts B. 2007. Observations of cell cluster hollowing in Staphylococcus epidermidis biofilms. Lett Appl Microbiol in press.
Telgmann U, Horn H, Morgenroth E. 2004. Influence of growth history on sloughing and erosion from biofilms. Water Res 38(17):3671–3684.
Thormann KM, Saville RM, Shukla S, Spormann AM. 2005. Induction of rapid detachment in Shewanella oneidensis MR-1 biofilms. J Bacteriol 187(3):1014–1021.
Thormann KM, Duttler S, Saville RM, Hyodo M, Shukla S, Hayakawa Y, Spormann AM. 2006. Control of formation and cellular detachment from Shewanella oneidensis MR-1 biofilms by cyclic di-GMP. J Bacteriol 188(7):2681–2691.
Trulear MG, Characklis WG. 1982. Dynamics of biofilm processes. J Water Pollut Control Fed 54(9):1288–1301.
Turakhia MH, Cooksey KE, Characklis WG. 1983. Influence of a calcium-specific chelant on biofilm removal. Appl Environ Microbiol 46(5):1236–1238.
Van der Borden AJ, van der Mei HC, Busscher HJ. 2005. Electric block current induced detachment from surgical stainless steel and decreased viability of Staphylococcus epidermidis. Biomaterials 26(33):6731–6735.
van Loosdrecht MCM, Salem S. 2006. Biological treatment of sludge digester liquids. Water Sci Technol 53(12):11–20.
Vuong C, Kocianova S, Yao YF, Carmody AB, Otto M. 2004. Increased colonization of indwelling medical devices by quorum-sensing mutants of Staphylococcus epidermidis in vivo. J Infect Dis 190(8):1498–1505.
Wanner O, Gujer W. 1986. A multispecies biofilm model. Biotechnol Bioeng 28(3):314–328.
Webb JS, Thompson LS, James S, Charlton T, Tolker-Nielsen T, Koch B, Givskov M, Kjelleberg S. 2003. Cell death in Pseudomonas aeruginosa biofilm development. J Bacteriol 185:4585–4592.
Wilson S, Hamilton MA, Hamilton GC, Schumann MR, Stoodley P. 2004. Statistical quantification of detachment rates and size distributions of cell clumps from wild-type (PAO1) and cell signaling mutant (JP1) Pseudomonas aeruginosa biofilms. Appl Environ Microbiol 70(10): 5847–5852.
Wimpenny JWT, Colasanti R. 1997. A unifying hypothesis for the structure of microbial biofilms based on cellular automaton models. FEMS Microbiol Ecol 22:1–16.
Xavier JB, Picioreanu C, Rani SA, van Loosdrecht MCM, Stewart PS. 2005. Biofilm-control strategies based on enzymic disruption of the extracellular polymeric substance matrix—A modelling study. Microbiol 151:3817–3832.
Xavier JB, Picioreanu C, van Loosdrecht MCM. 2005a. A framework for multidimensional modeling of activity and structure of multispecies biofilms. Environ Microbiol 7:1085–1103.
Xavier JD, Picioreanu C, van Loosdrecht MCM. 2005b. A general description of detachment for multidimensional modelling of biofilms. Biotechnol Bioeng 91(6):651–669.

DOI 10.1002/bit